FABRICATION OF APCVD PSG EMITTER-BASED INDUSTRIAL PERC SOLAR CELLS REACHING > 21.0% CONVERSION EFFICIENCIES

B. Kafle[1], P. Saint-Cast[1], U. Belledin[1], S. Lohmüller (née Werner)[1], H. Zunft[2], H. Knauss[2], P. Palinginis[3], C. Kusterer[3], R. Köhler[3], Thomas Zehl[3], A. Wolf[1], M. Hofmann[1]

[1]Fraunhofer Institute for Solar Energy Systems ISE, Heidenhofstr. 2, 79110 Freiburg, Germany
[2]Schmid, Gebr. Schmid GmbH, Robert-Bosch-Str. 32–36, 72250 Freudenstadt, Germany
[3]SolarWorld Industries GmbH, Am Junger-Löwe-Schacht 2, Freiberg, Germany

Correspondence: bishal.kafle@ise.fraunhofer.de, +49 (0) 761 4588-5499

ABSTRACT

Atmospheric pressure chemical vapour deposition (APCVD) of phosphosilicate glass (PSG) layer allows a separation of glass deposition and phosphorous diffusion step. This permits the application of the selective laser-doping process either before or after the thermal diffusion, which increases the freedom of tailoring the doping profiles of both lowly and highly doped regions of selective emitter structures. We fabricate industrial *p*-type PERC solar cells featuring APCVD PSG-based selective emitters and study the effect of laser-doping process on current-voltage characteristics. Mean conversion efficiency $\eta_{\text{mean}} = 21.1\%$ and an absolute gain $\Delta\eta_{\text{mean}} = 0.2\%$ to the homogeneous emitters is achieved for solar cells after applying the laser-doping process either before or after the thermal drive-in. The most promising selective emitter group is the one featuring the laser process before the thermal diffusion step, where a carrier concentration profile with depth $d = 0.9$ µm as well as a low specific contact resistivity ($\rho_{\text{C,mean}} \approx 3$ mΩ cm^2) are achieved. The major electrical loss of this group is related to the spectral response, where a higher front-reflection and an increased recombination at the illuminated fraction of the highly doped region need to be minimized in order to further push the efficiency level to $\eta > 21.5\%$.

Keywords: Doping, Atmospheric pressure, PERC solar cells

1. INTRODUCTION

With a continuous improvement in electrical properties and reduction of production cost, passivated emitter and rear cell (PERC)-type solar cell concept is set to become the standard cell architecture in industrial production [1]. However, still the losses in emitter region account for a significant proportion of the total recombination losses in a PERC solar cell [2]. In order to further minimize the emitter-related recombination losses, selective-emitter approaches are being increasingly adopted as it allows diffusion of an emitter with low surface concentration and thus, low saturation current density between the fingers ($j_{0,\text{pass}}$), whereas facilitating a lower contact resistivity (ρ_C) in contact areas. Additionally, another goal of the selective emitter approach is to minimize the recombination of minority charge carriers, i.e. lowering the saturation current density $j_{0,\text{met}}$ in the metallized area of the solar cell. Two of the major ways to achieve this are: a) formation of highly doped n^{++} areas under metal contacts for effective shielding of minority charge carriers towards reaching the contact area, b) minimizing the laser-induced damage in the Si lattice.

Meanwhile, the choice of the dopant source and the applied selective laser process can have a substantial effect on the resulting recombination as well as on the final contact resistance values of screen printed silver contacts. Typically, a phosphosilicate glass (PSG) layer formed by $POCl_3$-based tube diffusion process is used as the doping source to form laser-doped selective emitter regions [3]. In this study, we choose atmospheric pressure chemical vapour deposition (APCVD) as the technology to deposit phosphosilicate glass (PSG) layers on the Si surface. Apart from the economic potential of this technology compared to the conventional $POCl_3$-based tube furnace diffusion, its choice for this study is mainly due to: a) convenience of depositing single layer or stack of PSG glass with desired P concentration, and b) separation of glass (dopant source) deposition and thermal diffusion steps. The latter allows a freedom of tailoring doping profiles by independently varying the PSG deposition, laser and thermal diffusion steps, aiming to strike a balance between strong P diffusion and low laser-induced damage in the selective-emitter region.

One of the major barriers for the adoption of APCVD-based technology is a limited demonstration of high efficiencies using industrial-scale process steps. In this paper, we apply laser-based selective doping process on APCVD PSG layers, either directly after PSG deposition step or after the thermal diffusion step, and compare the electrical performances in the solar cell level. We start with electrical characterization of such selective n-type emitters on test structures using doping profiles and sheet resistance measurements. Afterwards, we apply APCVD PSG-based selective-emitter technology on large-area industrially fabricated *p*-type PERC solar cells and discuss the current-voltage characteristics of different groups.

2. EXPERIMENTAL

Figure 1 shows the experimental process plan followed to prepare PERC-type solar cells using APCVD-deposited PSG layer as the doping source. Alkaline textured *p*-type Czochralski (CZ) monocrystalline Si wafers with 1-3 Ω cm resistivity and edge length of 156 mm are used as precursor wafers. After HF-dip and DI-water rinsing, an inline APCVD deposition tool from SCHMID Thermal System Inc. is used to deposit a PSG layer stack on the textured side of the wafers. During the APCVD process, single doped layer or a stack of doped layer capped with a diffusion barrier layer (SiO_x) can be deposited in a single continuous run through the multiple deposition chambers. PSG layer deposition is performed by injecting N_2-diluted SiH_4, PH_3 and O_2 through the CVD injectors [4].

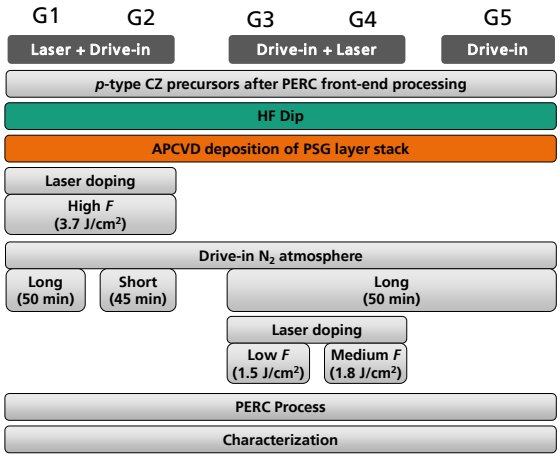

Figure 1: Experimental plan used to fabricate APCVD PSG-based CZ-PERC type solar cells. APCVD deposition of PSG layer stack is performed at Schmid GmbH, whereas laser doping, thermal diffusion and rest of the PERC processing steps are performed at SolarWorld Industries GmbH.

The concentration of P in the PSG layer mainly depends upon the gas flows and can be set as an input process parameter [5]. The gas flows are varied to form PSG layers of different P concentrations as well as to form un-doped barrier layers (SiO_x). Here, a stack of low concentration PSG/SiO_x/ high concentration PSG/SiO_x layers is deposited. The choice of phosphorous concentration in the PSG layers is made based upon our extensive study dedicated to the development of the homogeneous and selective emitters using APCVD PSG layer, and is discussed in another parallel conference paper [6].

Afterwards, highly doped regions are selectively formed either by applying laser-doping process before (*laser diffusion + drive-in*), or after (*drive-in + laser diffusion*) thermal diffusion at SolarWorld Industries GmbH. Groups G1 and G2 received *laser diffusion + drive-in* process, and differ only by the duration of the thermal drive-in process from each other. Groups G3 and G4 received *drive-in + laser diffusion* process, and differ only by the fluence (F) applied during the laser-doping process. Thermal drive-in process is performed under N_2 atmosphere in a tube furnace for 50 minutes in case of G1, G3, G4 and G5; whereas G2 received a shorter drive-in duration of 45 minutes.

In case of *laser diffusion + drive-in*, the laser process with a fluence of 3.7 J/cm^2 and pulse overlap of 100% is chosen based upon our past experience of this process leading to a low contact resistivity (ρ_C). For groups that received *drive-in + laser diffusion*, we choose two values of laser fluences (1.5 J/cm^2 for G3, 1.8 J/cm^2 for G4) for the solar cell precursors.

Please note that the selective laser-doping is applied only underneath the intended area for fingers and busbars for the solar cell precursors of G1-G4. For reference purpose, homogeneous emitter is formed for G5 without any laser doping. In parallel, characterization samples with laser fields are also prepared, where laser doping is performed in a larger area that can be used to measure doping profiles and emitter sheet resistances (R_{SH}) of both lowly and highly doped regions. Carrier concentration profiles are measured by using electro-capacitance-voltage (ECV) method on alkaline-textured samples and the profiles are corrected by adapting the surface factor that the sheet resistance determined from the charge carrier profile matches the sheet resistance measured by using four point probe (4pp) method [7,8].

After completing the diffusion processes, PSG etching is performed and the standard PERC fabrication sequence is followed for the solar cell precursors in the pilot line of SolarWorld Industries GmbH. It should be noted that the highly doped n^{++} region and the screen-printed metallization of the Ag grid are aligned for the selective emitter groups. In order to keep a tolerance for alignment, the selective-doping is performed in broader area than the width of the screen-printed fingers. The fraction of illuminated area with high doping to the total area of the solar cell is close to 6%, and the total metallization fraction is close to 4.5%. The screen-printing of rear and front sides is performed by using commercially available pastes, followed by a variation in the contact-firing process. *I-V* characteristics and spectral response of solar cells are measured after the regeneration process.

3. RESULTS AND DISCUSSION

3.1 Doping profiles of homogeneous and laser-doped emitters

Figure 2 shows the measured carrier concentration profiles of laser-doped emitters used in G1, G3 and G4, which received identical drive-in process (850°C, N_2 atmosphere, 50 min.). For comparison, doping profile of the homogeneous emitter that received no laser process (G5), is plotted as well. Please note that since G1 and G2 differ slightly in the drive-in duration, G2 is expected to have lower total phosphorous dose than G1 (profile not measured here). The corresponding emitter characteristics are listed in Table 1.

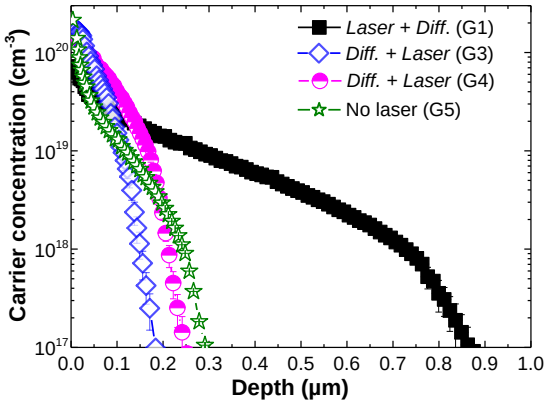

Figure 2: Carrier concentration measured by ECV for the homogeneous and selective doping processes applied in the solar cell batch measured on textured surface. The profiles are corrected by a surface factor to match the sheet resistance measured by 4pp.

For the interpretation of the carrier concentration profile, it should be noted that a significantly higher laser fluence is used for *laser diffusion + drive-in* group (G1,G2) in comparison to groups featuring *drive-in + laser diffusion* (G3,G4). In Figure 2, *laser diffusion + drive-in* group G1 leads to a lower N_S in comparison to the *drive-in + laser diffusion* selective

doping processes (G3/G4). For G3, the depth measured by ECV is lower than that of the homogeneous emitter (G5), which could be related to the slight differences in PSG layer thicknesses within the test wafer on which laser fields were prepared to perform ECV measurements.

Table 1: Characteristics of selective (laser-doped) and homogeneous emitters used in the solar cell batch, which are subjected to identical drive-in duration of 50 minutes. Emitter depths (d) are measured at 10^{16} cm^{-3} after linear extrapolation.

Doping process	Gr.	R_{SH} (Ω/□)	N_S (10^{20} cm^{-3})	d (nm)
laser + drive-in	G1	67	0.72	1000
drive-in + laser	G3	95	1.7	225
drive-in + laser	G4	73	1.75	290
drive-in	G5	119	2.0	320

In fact, *drive-in + laser diffusion* mainly increases the the near-surface emitter doping in comparison to the emitter formed without any laser-doping. Nevertheless, the thermally diffused emitter also features a high N_S, although a very steep decline in P concentration in the depth of the emitter. Moreover, applying *laser diffusion + drive-in* process leads to a significantly deeper profile ($d \approx 1$ µm) with an extended depth of the highly doped region ([P] > 10^{19} cm^{-3}) in comparison to the highly doped areas formed by *drive-in + laser diffusion* groups and to the emitter formed only by thermal *drive-in*. The differences in profile of selectively doped regions based on whether the laser doping is applied before or after the laser doping process is expected to be related to an easier access to a rich P source (PSG layer with [P]=20%) during drive-in process in the former case. Further studies are needed in order to understand the exact mechanism of dopant diffusion from such a stack of PSG layers.

Nevertheless, in case of a thick stack like the one used in this experiment, significantly higher laser fluences are required to induce dopant diffusion into Si for the group *laser diffusion +drive-in* in comparison to the *drive-in + laser diffusion*. Therefore, collective optimization of the layer stack (thickness and P concentration) and the laser process is worthwhile to investigate for such a diffusion process. In case of *drive-in + laser diffusion*, lower laser fluences are required to reach an equivalent value of R_{SH}. A full investigation of applying *laser + drive-in* and *drive-in + laser* processes for various laser fluences and evaluating the resulting doping profiles and the corresponding electrical parameters is out of scope of this paper and will be discussed in a future publication.

3.2 Solar cell results

I-V characteristics of the PERC-type solar cells are plotted in Figure 3. Excellent open-circuit voltages (V_{OC}) above 670 mV and a gain in V_{OC} compared to the homogeneous emitter (G5) is achieved for best groups of both types of selective emitter cells.

For *laser diffusion + drive-in* group, an advantage of shorter drive-in duration (G2) is observed in both V_{OC} ($\Delta V_{OC} \approx 2$ mV) and short circuit current density (J_{SC}) ($\Delta J_{SC} \approx 0.1$ mA/cm^2) of the solar cells. It should be noted that for a shorter drive-in duration (45 minutes), a higher average sheet resistance $R_{SH,mean} \approx 134$ Ω/□ is measured for the illuminated emitter in comparison to the longer drive-in duration of 50 minutes ($R_{SH,mean} \approx 120$ Ω/□). Hence, we attribute the gain in V_{OC} for G2 to a lower Auger recombination in the emitter in comparison to G1.

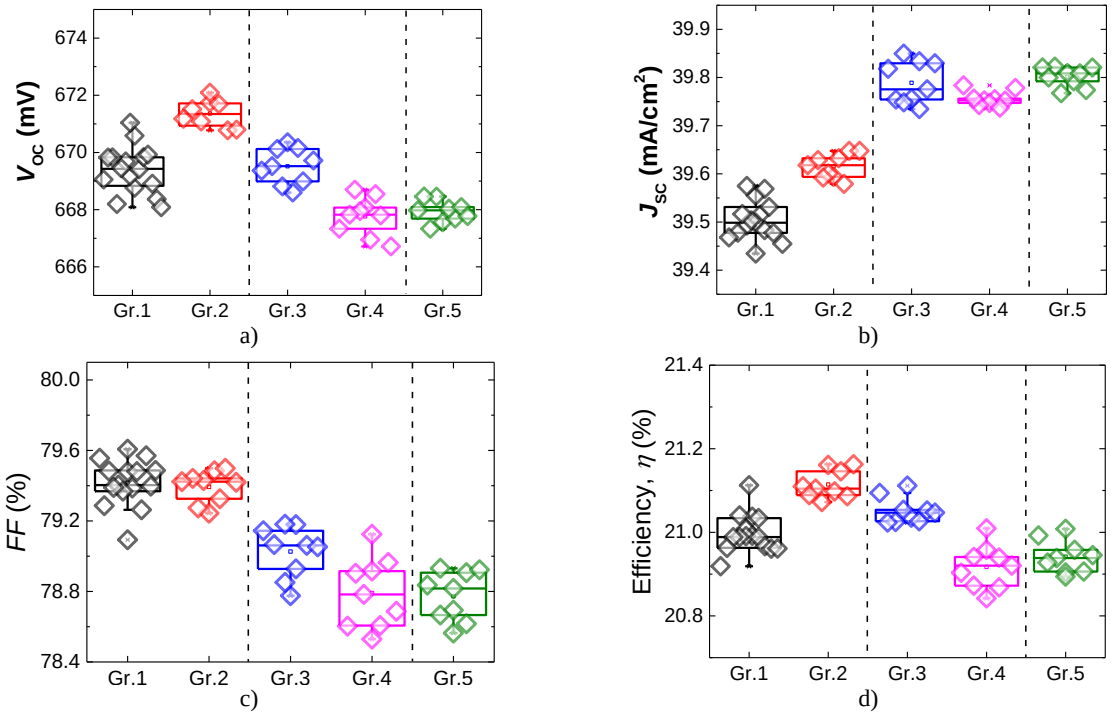

Figure 3: Illuminated *I-V* characteristics of the large area (156 mm edge length) *p*-type CZ PERC-solar cells measured in stable regenerated state, by using industrial cell tester with the reference cell calibrated to Fraunhofer ISE Callab.

In general, the solar cells that feature *laser diffusion + drive-in* show a significant loss in J_{SC} in comparison to other selective or homogeneous emitter solar cell groups. The reason for this will be discussed in the latter part of the paper. The solar cells featuring *laser diffusion + drive-in* (G1, G2) show a significantly higher fill factor (*FF*) in comparison to *drive-in + laser diffusion* (G3, G4) and the homogeneous emitter (G5). For *drive-in + laser diffusion* group, lower laser fluence of 1.5 J/cm^2 (G3) leads to a higher *FF* in comparison to a higher fluence of 1.8 J/cm^2 (G4). Overall, mean conversion efficiencies, $\eta_{mean} \geq 21.1\%$ is achieved for best selective emitter groups G1, G2 and G3. The champion solar cell from G2 reached 21.2% conversion efficiency. In comparison, homogeneous emitter solar cell group reached $\eta_{mean} = 20.9\%$.

3.3 Losses in selective-emitter solar cells

3.3.1 *FF* losses

The APCVD PSG-based selective-emitter groups reached higher *FF* than the homogeneous emitter group of solar cells. However, the *FF* values achieved in this solar cell batch are still lower than the expected values. Therefore, APCVD-based solar cells still have potential to reach higher *FF* and η if these losses can be minimized. To quantify the losses, a *FF* loss analysis is performed based upon the following measured parameters: a) *FF* from illuminated *I-V* curve, b) ideal value of fill factor FF_0 [9] that consists of only losses due to the first diode recombination parameter J_{01} and c) pseudo fill factor (*pFF*) from Suns-V_{OC} measurements that is free of series resistance (R_S) related losses [10]. By using these parameters, it is possible to identify the limiting loss-factors in *FF* of the solar cell. For example, *pFF-FF* provides a direct measure of R_S-related losses, whereas FF_0-*pFF* gives the extent of *FF* losses due to parallel resistance (R_P) and non-ideal recombination losses usually lumped in a second diode recombination parameter j_{02}. Furthermore, specific contact resistivity (ρ_C) is measured for two cells of each group (9 measurements per sample) using transmission line model (TLM) [11]. The parameters used to identify *FF*-losses in different solar cell groups are plotted in Figure 4.

Figure 4 a) shows the results for the *FF* loss analysis. It suggests that the selective emitter solar cells featuring *laser diffusion + drive in* are not limited by the R_S-related losses. It is also confirmed by a low mean value of specific contact resistivity $\rho_{C,mean}$=2.5 mΩ cm^2 for both G1 and G2 (see Figure 4 d)). In contrast, selective emitter solar cells featuring *drive-in + laser diffusion* are expected to be limited by R_S-related losses, mainly due to a higher value of ρ_C. We also confirmed that all groups have comparable values of Ag-grid related resistance losses.

Comparing Figure 4 d) with the carrier concentration profiles in Figure 2, one should notice that the behaviour is complex and cannot be reduced to a simple relation of ρ_C and N_S. In this study, the lowest ρ_C values are not obtained for emitter with high N_S value. Here, the shape of the profile and possibly the surface roughness left after the laser process is expected to have a large influence on the contacting property. In Figure 4 b), all groups show an equivalent value of FF_0-*pFF*, whereas as per Figure 4 a), losses due to R_P can be neglected for all groups (R_P > 10k Ω cm^2).

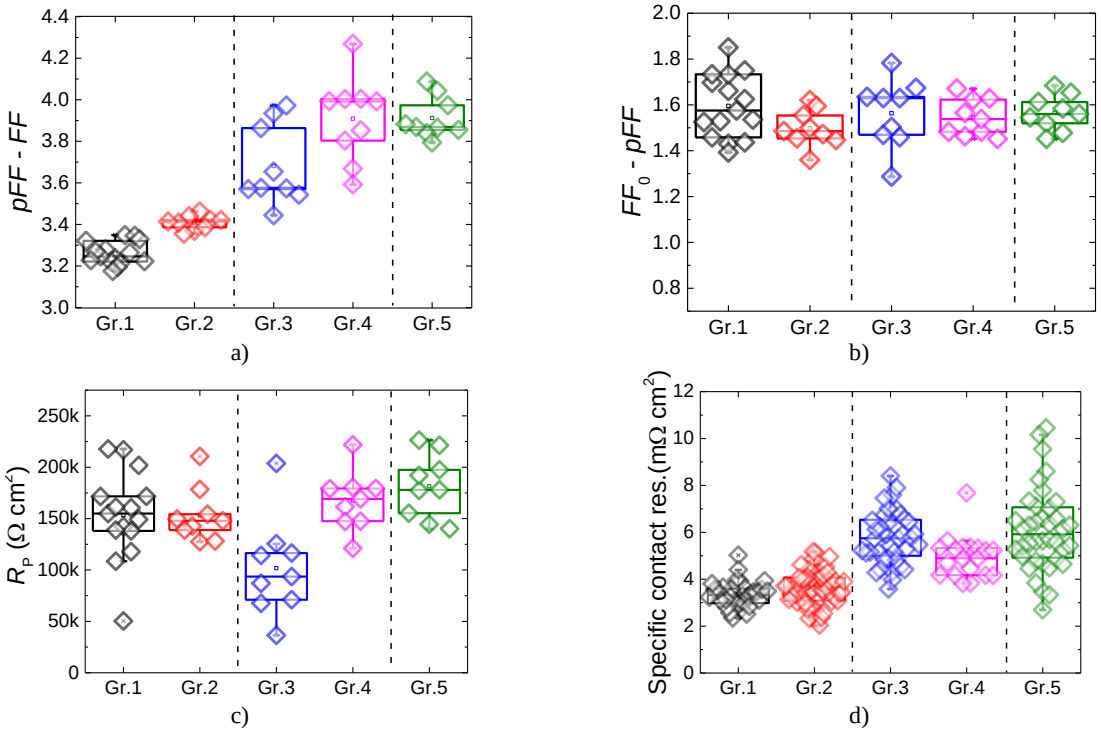

Figure 4: Plots comparing: a) *pFF-FF*, b) FF_0-*pFF*, c) parallel resistance (R_P) and d) TLM-measured contact resistivity (ρ_C) values of different solar cell groups.

In Figure 5, breakdown of j_{01}-limited *FF* (FF_0) of APCVD PSG-based solar cells, which followed either *laser + drive-in*, *drive-in + laser* or only *drive-in* processes are compared. APCVD-PSG based selective-emitter and homogeneous emitter solar cell groups clearly show high non-ideal recombination or j_{02}-related *FF* losses. Such j_{02}-related losses are generally related to the recombination losses in abrupt junctions, space charge region and other injection dependent recombination. In our case, origin of this loss in not yet completely understood, but expected to be related with impurity contamination during cell-processing steps and/or the wafer transport between different laboratories. As the rear-side of all solar cells are identically processed, the losses should be related to the front-side processing steps. In case of laser-doped emitters, this negative impact of j_{02} is expected to be compensated to some extent by the better shielding of minority charge carriers in the contact area, i.e. lower $j_{0e,met}$.

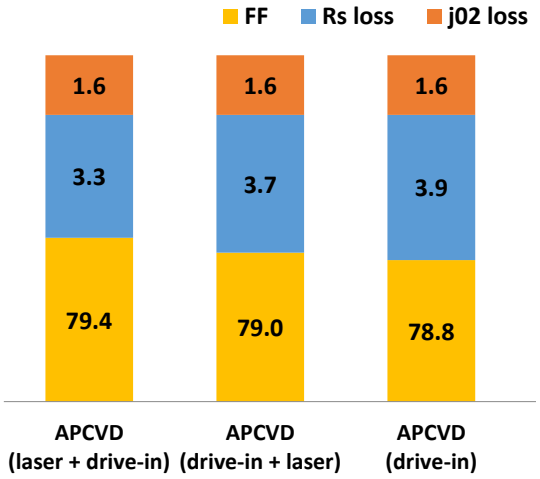

Figure 5: Breakdown of ideal *FF* (FF_0) into measured *FF* and losses due to series resistance (R_S) and recombination related to the second diode component (j_{02}). No significant losses occurred due to parallel resistance (R_P) on all solar cell groups.

Nevertheless, the j_{01}-limited *FF* or FF_0 of all APCVD-based PERC solar cell groups are identical. Furthermore, APCVD-group featuring *laser +drive-in* shows lowest R_S-related loss. The homogeneous emitter group shows the highest R_S-related losses that can be directly correlated to high contact resistivity values (see Figure 4 d)).

3.3.2 J_{SC} losses for *laser diffusion + drive in* group

In Figure 3 b), the groups featuring laser doping before thermal diffusion process show significant loss in J_{SC} in comparison to other groups In order to understand the losses, a schematic showing a unit area of the front side of a selective emitter solar cell is shown in Figure 6.

In Figure 6, w_{high} and w represent the width of selectively highly doped area and that of the screen-printed metal finger, respectively. The alignment tolerances lead to a laser-dope area where the highly doped area is not completely placed under the metal contact and therefore also participates in the charge carrier generation as the lowly doped emitter. Looking at the carrier concentration profiles of highly doped region for *laser + drive-in* group, one can expect a significantly higher Auger-related recombination in this region in comparison to the lowly-doped emitter. In combination with the much deeper junction, a notable loss in blue response is expected.

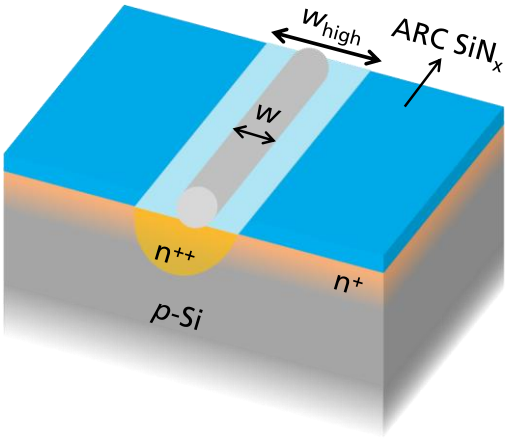

Figure 6: Schematic depicting the formation of selective emitter with a width w_{high} in the front-side of a solar cell, on which a Ag-grid with fingers of width w is printed.

In their studies, Jäger et al. argue that such Auger-related recombination losses forming dead layer in highly doped region is responsible for J_{SC} losses in selective-emitter solar cell that do not exhibit a perfect alignment between laser-doping and screen printing [12]. Apart from this, laser-induced defects can also activate Shockley Read Hall (SRH) recombination channel, although the consequent *drive-in* process is expected to anneal the defects to some extent. Meanwhile, higher and longer laser pulse energies could also significantly change the surface topography due to longer and deeper melting and crystallization phases of Si substrate. Thus, apart from the recombination losses that are typically visible in the internal quantum efficiency (*IQE*) of solar cells, losses in external quantum efficiency (*EQE*) due to a higher reflection of the illuminated highly doped area can also influence J_{SC}. This effect is often neglected for conventionally applied selective-doping processes; however, it demands a closer look if high laser fluences and overlaps are used as in the case of G1 and G2.

EQE and *IQE* measurements are performed for the solar cells from groups G1 and G5. These groups are chosen as they showed respectively the minimum and maximum J_{SC} of all groups, and therefore are expected to allow a better understanding of losses that are limiting J_{SC} of groups G1 and G2. The front reflection-related losses in J_{SC} for each group is calculated by using measured *IQE* and front-reflection of the solar cell using the AM 1.5 spectrum as described in [13,14]. Recombination related losses in J_{SC} are extracted based upon deviation of measured *IQE* to the ideal case, using the model of Fischer [15] as explained in [14]. J_{SC}-losses calculated for selective-emitter solar cell (G1) and homogeneous-emitter solar cell (G5) are shown in Figure 7.

The chart suggests that for higher laser fluences as used in the selective emitter solar cell group featuring *laser + drive-in* (G1), reflection-related losses can be as significant as the recombination related losses in the final J_{SC} value of a selective emitter solar cell. The model suggests higher shading losses for G1 in comparison to

G5. This could be related to a change in surface topography due to the laser-doping process, which is also suggested by a higher reflection-related J_{SC} loss for G1 in comparison to G5. Higher laser fluence is most likely to deform the surface texture due to a longer melting of Si [16], thereby changing the wetting and flow behaviour of the Ag-paste on Si surface, leading to a higher paste bleeding during the screen-printing process. Further characterization of the contact geometry on differently lasered surfaces is necessary in order to prove this hypothesis.

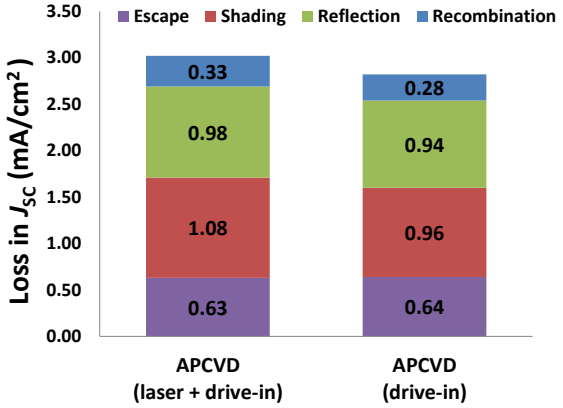

Figure 7: Loss in J_{SC} in the selective emitter solar cell group G1 (left) and the homogeneous emitter solar cell group G5 (right), due to recombination in the emitter region, front-reflection losses, shading due to metal contacts and escape reflection-related losses.

4. SUMMARY

We fabricated p-type CZ-PERC selective emitter solar cells using APCVD-PSG layer as the doping source in industrial pilot cell fabrication line of the high volume manufacturer SolarWorld Industries GmbH. An APCVD tool produced by SCHMID Thermal System Inc. is used to deposit PSG and barrier layers. The APCVD technology allows the separation of PSG deposition and drive-in step in comparison to conventional selective emitter cells that use $POCl_3$ as the doping source. This allowed us to perform selective doping either before or after the thermal drive-in step. In first demonstration of this technology in high-efficiency PERC solar cells, conversion efficiencies of up to $\eta_{max} \approx 21.2\%$ are achieved. To the knowledge of authors, this is one of the most systematic applications of this technology on PERC-type solar cells that have demonstrated with high conversion efficiencies.

Both selective emitter groups (*laser + drive-in* & *drive-in + laser*) show an average efficiency improvement of 0.2% to the homogeneous emitter group. Solar cells featuring *laser + drive-in* are measured to have low ρ_C values ($\rho_{C,mean} \approx 3\ m\Omega\ cm^2$) and a deep carrier concentration profile ($d \approx 0.9\ \mu m$), hence show advantages in both V_{OC} and *FF* values to the homogeneous emitter group. In contrast, ρ_C-related R_S losses dominate the *FF* of *drive-in + laser* and further optimizations in layer properties and laser-doping are required. Significant non-linear recombination -related losses in *FF* and V_{OC} are observed for all APCVD-based solar cell groups. Finally, the J_{SC} loss of 0.2-0.3 mA/cm^2 for *laser + drive-in* groups is attributed to the illuminated fraction of the highly doped region of the selective-emitter solar cell. A loss analysis of J_{SC} using *QE* measurements suggests that for sufficiently higher laser fluences, contribution of front-reflection and metal shading is significant and should be also considered along with the usually reported Auger-related recombination in the illuminated fraction of the highly-doped emitter region.

5. ACKNOWLEDGEMENTS

This work is funded by the federal ministry for economic affairs and energy (BMWi) of Germany within the project APPI under the contract number 0325895A. Project APPI is supported under the umbrella of SOLAR-ERA.NET Cofund by Agence de l'Environnement et de la Maîtrise de l'Energie, Project management Jülich, Technology Strategy Board and Centro para el desarollo tecnológico. SOLAR-ERA.NET is supported by the European Commission within the EU Framework Programme for Research and Innovation HORIZON 2020 (Cofund ERA-NET Action, N° 691664). The authors would like to thank all co-workers at photovoltaics department of Fraunhofer ISE, especially Stefan Schmidt for ECV analysis, Sebastian Mack for helpful discussions, Eleni Miethig for help in solar cell processing; and Elisabeth Schaeffer, Felix Martin for their help in solar cell characterization.

6. REFERENCES

[1] International Technology Roadmap for Photovoltaic (ITRPV): 2017 Results including maturity report: Eighth edition, 2018.

[2] M. Müller, G. Fischer, B. Bitnar, S. Steckemetz, R. Schiepe, M. Mühlbauer, R. Köhler, P. Richter, C. Kusterer, A. Oehlke, E. Schneiderlöchner, H. Sträter, F. Wolny, M. Wagner, P. Palinginis, D.H. Neuhaus, Loss analysis of 22% efficient industrial PERC solar cells, Energy Procedia 124 (2017) 131–137.

[3] T.C. Röder, S.J. Eisele, P. Grabitz, C. Wagner, G. Kulushich, J.R. Köhler, J.H. Werner, Add-on laser tailored selective emitter solar cells, Prog. Photovolt: Res. Appl. 18 (7) (2010) 505–510.

[4] K.O. Davis, K. Jiang, C. Demberger, H. Zunft, H. Haverkamp, D. Habermann, W.V. Schoenfeld, Improved control of the phosphorous surface concentration during in-line diffusion of c-Si solar cells by APCVD, Phys. Status Solidi RRL 7 (5) (2013) 319–321.

[5] Felix Book, Holger Knauss, Carsten Demberger, Florian Mutter, Giso Hahn, Phosphorous Doping from APCVD Deposited PSG. in 32nd European Photovoltaic Solar Energy Conference and Exhibition (2016) 824–827.

[6] Pierre Saint-Cast, Udo Belledin, Elmar Lohmüller, Bishal Kafle, Julian Weber, Sven Seren, Andreas Wolf, Marc Hofmann, SELECTIVE EMITTER USING APCVD PSG LAYERS AS DOPING SOURCE, 34th EUPVSEC (this conference).

[7] Robert Bock, Pietro P. Altermatt and Jan Schmidt, Accurate extraction of doping profiles from Electrochemical capacitance voltage measurements, in 23rd EUPVSEC, Valencia, Spain (2008).

[8] Achim Kimmerle, Diffused surfaces for crystalline silicon solar cells - process development, characterization and modelling. Dissertation, Universtiy of Freiburg, Freiburg, Germany, 2015.

[9] M.A. Green, Solar cells: operating principles, technology, and system applications, Prentice-Hall, 1982.
[10] R. A. Sinton, A. Cuevas, A Quasi-Steady-State open-circuit voltage method for solar cell characterization, in 16th EUPVSEC, Glasgow, UK (2000).
[11] G. K. Reeves and H. B. Harrison, Obtaining the Specific Contact Resistance from Transmission Line Model Measurements, IEEE ELECTRON DEVICE LETTERS 3 (5) (1982) 111–113.
[12] U. Jäger, B. Thaidigsmann, M. Okanovic, R. Preu, Quantum Efficiency Analysis of Highly Doped Areas for Selective Emitter Solar Cells, Energy Procedia 8 (2011) 193–199.
[13] B. Thaidigsmann, A. Wolf, D. Biro, ACCURATE DETERMINATION OF THE IQE OF SCREEN PRINTED SILICON SOLAR CELLS BY ACCOUNTING FOR THE FINITE REFLECTANCE OF METAL CONTACTS, in 24th EUPVSEC, Hamburg, Germany (2009).
[14] B. Thaidigsmann, A. Wolf, F. Clement, D. Biro and R. Preu, COMBINING THE ADVANTAGES OF WRAP THROUGH METALLIZATION AND REAR SURFACE PASSIVATION INTO INDUSTRIAL MWT-PERC DEVICES. in 25th EUPVSEC, Valencia, Spain, 2010.
[15] B. Fischer. M. Keil, P. Fath, E. Bucher, Scanning IQE measurement for accurate current determination on very large area solar cells, Conference Record of the Twenty-Ninth IEEE Photovoltaic Specialists Conference, New Orleans, LA, USA (2002) 454–457.
[16] T. Röder, A. Esturo-Breton, S. Eisele, C. Wagner, J.R. Köhler, J.H. Werner, Fill Factor of Laser Doped Textured Silicon Solar Cells. 23rd European Photovoltaic Solar Energy Conference and Exhibition, Valencia, Spain 1-5 September (2008) 1740–1742.